International Space Planes and Hypersonic Systems and Technologies Conferences
6-9 March 2017, Xiamen, China
21st AIAA International Space Planes and Hypersonics Technologies Conference

Experimental Investigation of Fuel-Cooled Combustor: Cooling Efficiency and Coke Formation

L. Taddeo[1], N. Gascoin[2], K. Chetehouna[3]
INSA Centre Val de Loire, PRISME, 88 boulevard Lahitolle, Bourges, France

A. Ingenito[4], F. Stella[5]
Department of Mechanical and Aerospace Engineering, University of Rome "La Sapienza", Rome, Italy

and

M. Bouchez[6], B. Le Naour[7]
MBDA France, 8, rue Le Brix, 18000 Bourges, France

Scramjet is an air-breathing engine designed to propel advanced aircrafts in the atmosphere, suitable, according to various studies, to thrust high-speed hypersonic flights (over Mach 5). The thermal protection of vehicles flying at hypersonic velocities is a critical problem; as at supersonic speeds the incoming air is at too high temperature to be used as a coolant, the fuel becomes the only adequate source of cooling for the vehicle. Regenerative cooling is a well-known cooling technique using the fuel as coolant. As the development of regeneratively cooled engines faces many difficulties, an empirical study of this cooling technology and of its complex dynamics is of high interest. In this context, a remotely controlled fuel-cooled combustor, suitable for the experimental analysis of the pyrolysis-combustion coupling characterizing a fuel-cooled combustion chamber when a hydrocarbon propellant is used, has been designed. Tests are realized under both stationary and transient conditions using ethylene as fuel and air as oxidizer. Two operating parameters, i.e. fuel mass flow rate (between 0.010 and 0.040 g.s^{-1}) and equivalence ratio (between 1.0 and 1.5), have been investigated. It has been observed that fuel mass flow rate increases always result in the raise of the heat flux density passing from the combustion gases to the combustor walls. It has been seen that mass flow rate raises between 16 and 20 % lead to increases in the thermal energy evacuated by the fuel-coolant in the range from 30.4 to 48.5 %, depending on equivalence ratio and pressure. The dependence of the cooling system heat exchange efficiency on the two operating parameters has been demonstrated. The consequences of the coking activity of the fuel have also been investigated. For applied interest, a monitoring method for carbon deposits formation has been developed and validated.

Nomenclature

A	=	surface
c_1	=	numerical constant
c_2	=	numerical constant
C_p	=	heat capacity
D	=	diameter
ΔP	=	pressure drop
F	=	view factor

[1] PhD Student, Pyrolysis & Propulsion Group, lucio.taddeo@insa-cvl.fr
[2] Full Professor, Pyrolysis & Propulsion Group, Senior AIAA Member, nicolas.gascoin@insa-cvl.fr
[3] Tenure Professor, Pyrolysis & Propulsion Group, khaled.chetehouna@insa-cvl.fr
[4] Researcher, AIAA Member
[5] Full Professor
[6] Senior Expert, AIAA Member
[7] Application Engineer

f_v = volume fraction
h = convective heat transfer coefficient
H = height
k = thermal conductivity
L = length
$\dot{m}$ = mass flow rate
P = pressure
q = heat flux density
S = cross section
t = time
T = temperature
v = velocity

Greek Symbols

ε = emissivity
η = efficiency
μ = dynamic viscosity
ρ = density
σ = Boltzmann's constant
φ = equivalence ratio of fuel to oxidizer

Subscripts

amb = ambient conditions
cc = cooling channel
conv = convective
comb = combustor
ext = combustor external wall
f = fuel
g = combustion gases
int = combustor internal wall
rad = radiative
th = thermocouple

I. Introduction

The development of aircrafts and space vehicles able to achieve hypersonic velocities (over Mach 5) may provide significant commercial benefits. Indeed, hypersonic flight is suitable for both civil and military applications, as the development of hypersonic aircrafts and hypersonic missiles[1]. Because of the operational limitation of gas turbine engines to speeds generally under Mach 4, high-speed flight propulsion systems must integrate engines capable of propelling the vehicle when its velocity becomes hypersonic. To this end, Scramjets represent a very effective solution. Scramjets are air-breathing jet engines suitable for atmospheric flight, using ambient air as oxidizer. Incoming air enters the air inlet at very high speed and is compressed thanks to the forward motion of the vehicle, without any rotary compressor. Scramjets are, according to various studies, suitable to thrust missiles and aircrafts and even reusable space transport vehicles at speeds between Mach 4 and Mach 10, where their specific impulse is unmatched[2-4].

At hypersonic speeds, vehicle thermal protection becomes critical, particularly with respect to the engine combustion chamber, which is exposed to very high temperatures. At Mach 8, for example, combustion gases total adiabatic temperature can achieve 4500 K, far in excess of all known structural material capability[5-7]. Several cooling techniques can be used to protect the combustor internal surfaces from the hot combustion gases. In general, when the operating time of the vehicle is not in the order of few minutes, active cooling techniques, requiring the use of a coolant, must be implemented. In this sense, when compared to air, fuels are generally much better coolants; at hypersonic speeds, the fuel becomes the only adequate source of cooling for the vehicle[7-11].

Regenerative cooling is a cooling technique using the fuel as coolant. Indeed, before being burned, the propellant flows through cooling channels located between the inner and the outer walls of the engine. Thus, a counter-flow heat exchange between the fuel-coolant and the burned gases is generated and combustor internal surfaces are cooled[5,12,13]. Regenerative cooling is particularly effective when an endothermic fuel is used, as, when heated at high temperatures,

endothermic hydrocarbons undergo endothermic thermal decomposition. That enhances their cooling capability[7]. Moreover, fuel decomposition in the cooling channels generates light hydrocarbons, whose ignition delay times are much lower than that of the original propellant; therefore fuel combustion kinetics become faster and the performance of the engine improves[12,13]. This is a key benefit of this cooling technology, as one of the weak points of Scramjets engines, deriving from the very low time that the fuel and the oxidizer spend in the combustor (in the order of few ms[12]), is the difficulty to complete fuel combustion in the combustion chamber.

The design of regeneratively cooled Scramjets is a challenging task, facing several difficulties. Some of the most relevant issues concerning the development of fuel-cooled Scramjets have already been studied in the framework of various programs. Several numerical studies have been performed to evaluate the heat flux densities between the combustion gases and the combustor internal surfaces and to identify the highest heat flux combustor regions[4,8,14-18]. The design of the cooling channels has been the subject of many works; the effects of their shape and of their cross-section area on combustion chamber walls temperature and on fuel-coolant temperature and pressure drop have been thoroughly investigated[19-23]. The possibility of employing carbon composite materials for the manufacturing of the combustor walls has been thoroughly studied[24-26]. Several studies have also been realized on endothermic hydrocarbons thermal decomposition, aiming at determining the main products for various jet fuels and for various operating conditions of pressure, temperature or residence time[27-30].

A particular attention has been paid to the study of the coking activity characterizing hydrocarbon fuels high-temperature decomposition. Indeed, as hydrocarbons thermal pyrolysis mainly results in the formation of species as hydrogen, ethylene and ethane, which are highly hydrogenated, fuel decomposition in the cooling channels of a fuel-cooled combustor can lead to the formation of carbon depositions. This phenomenon raises serious concerns, especially if very long system lifetimes are required, for its negative consequences: 1) decrease in the heat transfer efficiency of the overall cooling system (due to thermal insulation of carbon, whose thermal conductivity is 4 to 6 times less than that of steel metallic materials); 2) decrease in the endothermicity of fuel decomposition reactions; 3) increase in the pressure drop or even system failure due to cooling channels or fuel injectors obstruction[7,31-34].

However, to the author's knowledge, none of published studies focused on the most important aspect characterizing regeneratively cooled combustors, i.e. the strong coupling between fuel decomposition and fuel combustion, which makes the definition of a control strategy for this type of engines a major challenge. Even the effect on engine thrust of the most important operating parameter, i.e. the mass flow rate of the fuel fed to the engine, is not easy to determine. Indeed, engine thrust depends both upon fuel mass flow rate and fuel composition, which are linked to each other, as fuel composition vary with fuel residence time in the cooling channels that, in turn, vary with fuel mass flow rate. A mass flow rate increase would probably result in a residence time decrease and, consequently, in a less enhanced fuel decomposition. Thus, the propellant injected in the combustor would contain less low ignition delay time species; consequently, the global effect could even be a drop in the engine thrust or even flame extinction[12,13,35]. To the author's knowledge, the only work analysing this point is the one of Gascoin[12], in which the impact of fuel mass flow rate on burned gases temperature, fuel-coolant temperature and residence time in the cooling channels has partially been defined by means of numerical calculations.

The necessity of an empirical study of such a complex technology is evident; this is the only approach permitting to develop an engine control strategy suitable for on-board application on a hypersonic vehicle. The present work aims at validating experimentally the already acquired numerical knowledge of a regeneratively cooled combustor when a hydrocarbon is used as fuel. To this end, a remotely controlled combustor, suitable for the experimental analysis of a fuel-cooled engine, has been designed. The cooling channels typical of a fuel-cooled Scramjet have been re-created by means of a single rolled-up stainless steel tube which passes in the combustion chamber and is placed on the combustor internal wall. Experiments are performed under both stationary and transient conditions by using ethylene as fuel and air as oxidizer. Two command parameters, which are fuel mass flow rate $\dot{m}_f$ (in the range from 0.010 to 0.040 $g.s^{-1}$) and fuel to oxidiser equivalence ratio φ (in the range from 1.0 to 1.5) are investigated. Thanks to this innovative experimental set-up (extensively described in a previous work[13]), the effect of these two operating parameters on the main heat fluxes characterizing the combustor is analyzed. The variations of the convective and of the radiative heat fluxes passing from the burned gases to the combustor wall resulting from $\dot{m}_f$ and φ variations are examined. The sensible heat flux absorbed by the fuel-coolant is calculated. The heat transfer efficiency of the cooling system is determined. The coking activity of the fuel in the cooling channel is also investigated; a carbon deposition monitoring method, suitable for real-time on-board application, is proposed.

This work will raise the knowledge of the scientific community on the thermal management and control of a regeneratively cooled Scramjet.

II. Materials and Method

A. Description of the test bench

The experimental set-up consists in a fuel-cooled combustor which allows the experimental investigation of the coupling between fuel pyrolysis and fuel combustion occurring on fuel-cooled engine using an endothermic hydrocarbon propellant. It also permits to study the effects of the high-temperature coking activity of this type of fuels on the performace of the cooling system. The combustor, whose height is of 0.5 m, is composed of two stainless steel co-axial tubes having respectively a diameter of 0.1 m (the internal one) and of 0.3 m (the external one) and a thickness of 1 mm, separated by a ceramic insulation blanket. The cooling channels are reproduced by a single rolled-up stainless steel tube having a length of 40 m, whose internal and external diameters are respectively 1.0 mm and 3.2 mm. It passes in the combustion chamber entering from the top and exiting from the bottom and is placed on the internal wall of the combustor. Consequently, the fuel-coolant is exposed to the heat flux generated by the flame before being burned. A scheme of the combustor is represented in fig. 1. Its dimensions and characteristics have been computed in conformity with expected values on a real configuration by using similitude rules[13].

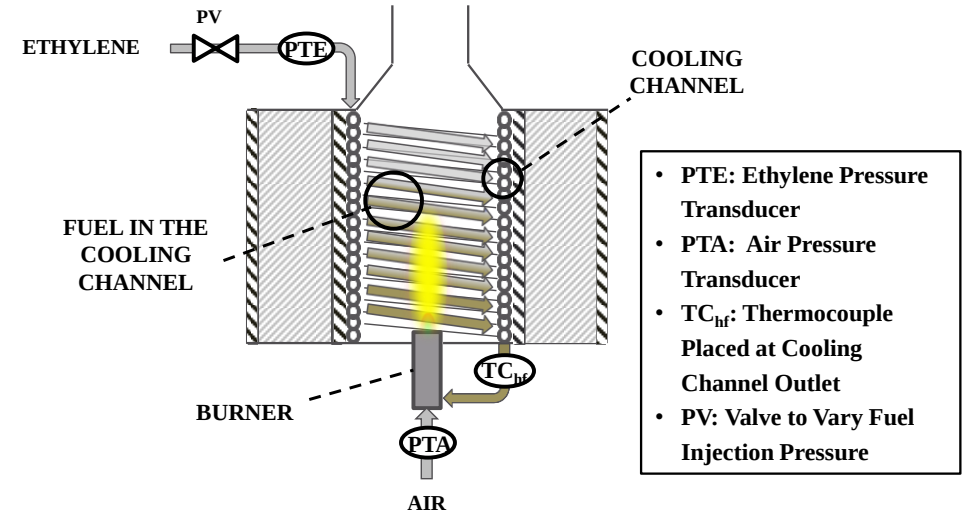

Figure 1. Scheme of the regenerative cooling combustion chamber

The fuel and the oxidizer used to carry out the tests, which are respectively ethylene and air, are fed to the combustor by using two high-precision mass flow controllers, respectively a Bronkhorst F-201CM-10K-RDA-88-K for ethylene (with a range of 0-0.2 g.s^{-1}) and a Bronkhorst F-202AV-M20-RDA-55-V for air (with a range of 0-5.0 g.s^{-1}). Two pressure transducers, indicated as PTE and PTA in fig. 1, are used to measure respectively the pressure of the ethylene entering the cooling channel and the pressure of the air entering the burner. The temperatures achieved by the burned gases are measured by eleven type K thermocouples, which can be shifted from the wall to the axis of the combustor. Their positions are shown in fig. 2, where the base of the combustion chamber is used as reference. A type K thermocouple (indicated as TC$_{hf}$ in fig. 2) is located at the outlet of the cooling channel from the combustor, to measure the temperature of the heated fuel.

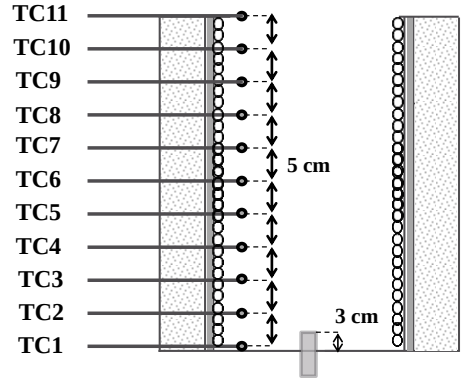

Figure 2. – Scheme representing the position of the thermocouples used to measure the combustion gases temperature field

The burner used to generate the flame is a Five North American SPB5 pilot burner, which permits to mix the fuel and the oxidizer in order to produce a pre-mixed combustion, having a nominal capacity of 6 kW. The choice of premixed flame allows to facilitate the numerical study of the system.

The experimental bench is completely automated. Further details on it have already been given in a previous work[13].

B. Test Methodology

Experiments are run by varying two operating parameters, i.e. fuel mass flow rate $\dot{m}_f$ (in the range from 0.01 to 0.04 $g.s^{-1}$) and equivalence ratio φ (in the range from 1.0 to 1.5), which is modified by varying the ratio between ethylene mass flow rate and air mass flow rate. A brief review of the test cases which have been realized is given in tab. 1.

Test Case	Fuel Mass Flow Rate ($g.s^{-1}$)	Equivalence Ratio	Fuel Inlet Pressure (Bar)
1	0.020-0.030-0.040	1.50	1.0
2	0.020-0.024-0.028	1.00	1.0
3	0.020-0.024-0.029	1.25	1.0
4	0.020-0.024-0.030	1.50	1.0
5	0.024	1.00-1.25-1.50	5.0
6	0.020-0.024-0.039	1.00	4.5
7	0.020-0.025-0.029	1.25	5.0
8	0.020-0.024-0.029	1.50	4.0
9	0.016	1.25	5.00-8.0-11.0

Table 1. – Overview of the test matrix summarizing the command parameters

Each experiment is carried out by varying a single input parameter, to investigate its effect on the dynamics of the combustor; during each test, this parameter is increased twice and then decreased twice, while keeping the other constant. Operating conditions are varied only when steady state has been achieved, i.e. when the rate of variation of the temperature of the fuel-coolant measured at the outlet of the cooling channel (thermocouple TC_{hf}) becomes lower than 0.1 $K.min^{-1}$. For example, let us consider the test case number 1 of tab. 1. The test is started with a fuel mass flow rate of 0.020 $g.s^{-1}$ and an equivalence ratio of 1.50; when steady state is achieved, fuel mass flow rate is increased from 0.020 to 0.030 $g.s^{-1}$ to let the system reach a new stationary state. Similarly, fuel mass flow rate is later increased to 0.040 $g{\cdot}s^{-1}$, then reduced twice respectively to 0.030 and 0.020 $g.s^{-1}$, to come back to the initial operating conditions. Meanwhile, fuel equivalence ratio is not modified. Thus, during each experiment, the test bench achieves steady state five times. For simplicity purposes, they will be numbered consecutively, beginning from steady state 1 and finishing with steady state 5.

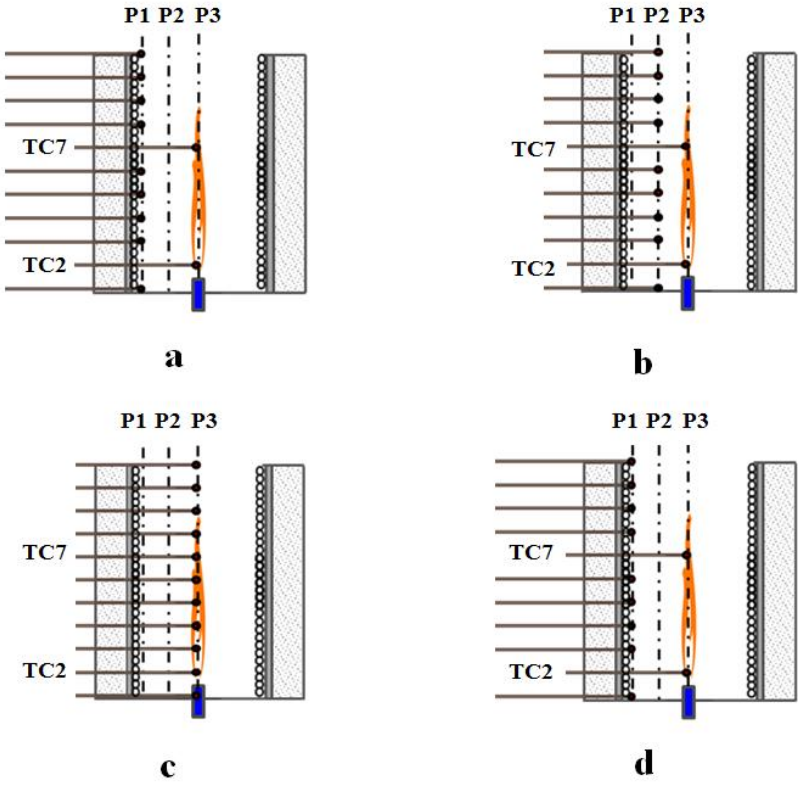

Figure 3. Test sequences (a to d) representing the different locations of thermocouples to monitor the temperature field in the combustor during the test

At the start of each test, all the thermocouples are placed at 1 cm from the wall of the combustor, at position P1, with the exception, of the two thermocouples indicated respectively as TC2 and TC7, which are placed at 5 cm from the wall, on the axis of the combustion chamber, at position P3 (fig. 3-a). When a steady state is achieved, the thermocouples which are at position P1 are first shifted at position P2 (at 3 cm from the wall, fig. 3-b), then at position P3, each time after the stabilization of the measured temperatures (fig.3-c). Before varying the input parameter whose effect is studied, the thermocouples which had been displaced are moved back to their original positions (fig. 3-d).

C. Data Post-Processing

The objectives of this work include the calculation of the heat load passing from the combustion gases to the combustor wall and the heat load absorbed by the fuel-coolant. The total heat flux density passing from the combustion gases to the combustor wall has been calculated using the following equation:

$$q_g = q_{g,conv} + q_{g,rad} \tag{1}$$

In equation (1), q_g is the total heat flux density passing from the burned gases to the combustion chamber internal surface, whereas $q_{g,conv}$ and $q_{g,rad}$ are respectively the convective and the radiative heat flux density. The following equation is used to calculate $q_{g,conv}$:

$$q_{g,conv} = h_g \cdot \left(T_{g,P3} - T_{g,P1}\right) \tag{2}$$

In the above equation, h_g is the convective heat transfer coefficient, $T_{g,P1}$ is the gas temperature measured in position P1 and $T_{g,P3}$ is the gas temperature measured in position P3. The convective heat transfer coefficient h_g is calculated using the following equation[36]:

$$h_g = 1.86 \cdot \frac{k_g}{D_{int}} \cdot \left(\frac{D_{int}}{H^*} \cdot Re_g \cdot Pr_g\right)^{0.33} \cdot \left(\frac{\mu_{g,P3}}{\mu_{g,P1}}\right)^{0.14} \tag{3}$$

where Re_g and Pr_g are defined as follows:

$$Re_g = \frac{\rho_g \cdot D_{int} \cdot v_g}{\mu_g} \tag{4}$$

$$Pr_g = \frac{C_{p,g} \cdot \mu_g}{k_g} \tag{5}$$

In equations from (3) to (5), k_g is the average gas thermal conductivity, ρ_g is the average gas density, μ_g is the average gas viscosity, $C_{p,g}$ is the average gas specific heat, v_g is the average gas velocity, D_{int} is the internal diameter of the combustor, H^* is a characteristic length (it is assumed to be one tenth of the combustor height), $\mu_{g,P1}$ is gas viscosity in position P1 and $\mu_{g,P3}$ is gas viscosity in position P3. The average value of each property is calculated at the average gas temperature between position P1, P2 and P3.

The following equation is used to calculate the radiative heat flux $q_{g,rad}$[36]:

$$q_{g,rad} = \varepsilon \cdot \sigma \cdot F \cdot \left({T_{g,P3}}^4 - {T_{g,P1}}^4\right) = \left(\varepsilon_g + \varepsilon_s - M \cdot \varepsilon_g \cdot \varepsilon_s\right) \cdot \sigma \cdot F \cdot \left({T_{g,P3}}^4 - {T_{g,P1}}^4\right) \tag{6}$$

where ε is flame emissivity, ε_g is the combustion gases emissivity, ε_s is the soot emissivity, σ is the Stefan–Boltzmann's constant and F is the view factor. The calculation of the emissivity of the combustion gases is based, depending upon the species, on the Hottel emissivity charts[37] and on the calculations of Malkmus and Thompson[36], whereas soot emissivity ε_s and the correction factor M are calculated by using the following equations[36]:

$$\varepsilon_s = 1 - (1 + c_1 \cdot f_{vol} \cdot L \cdot T_g \cdot {c_2}^{-1})^{-4} \tag{7}$$

$$M = 1.12 - 0.27 \cdot \frac{T_g}{1000} + 2.7 \cdot 10^5 \cdot f_{vol} \cdot L_{rad} \tag{8}$$

In equations (7) and (8), T_g is the gas temperature in degree Kelvin, f_{vol} is the soot volume fraction, L_{rad} is the path length of the radiation in m (it is assumed to be 0.058 m)[37], c_1 is an adimensional constant varying with fuel type (it is assumed to be 8.9)[38] and c_2 is Planck's second constant (it has a value of 0.0144 m·K)[36]. Soot volume fraction is estimated by using data kept from literature[39-41].

The following equation is used to calculate the sensible heat flux absorbed by the pyrolyzing fuel:

$$q_{f,cc} = \dot{m}_f \cdot C_{p,f} \cdot \left(T_{f,out} - T_{f,in}\right) \tag{9}$$

where $C_{p,f}$ is fuel specific heat, $T_{f,in}$ is fuel temperature at cooling channel inlet and $T_{f,out}$ is fuel temperature at cooling channel outlet, before its injection in the burner.

To characterize the performance of the regeneratively cooled combustor, the heat transfer efficiency of the overall cooling system has been calculated. It is defined as the ratio between the actual rate of heat transfer from the combustion gases to the coolant and the optimum one[42]:

$$\eta = \frac{q_{f,cc}}{q_{f,cc}\big|_{opt}} = \frac{q_{f,cc}}{U \cdot A_{int} \cdot \Delta T_{log}} \tag{10}$$

where the local overall heat-transfer coefficient U and the logarithmic mean temperature difference ΔT_{log} are calculated using the following equation[36]:

$$U = \left(\frac{1}{h_g} + \frac{1}{h_{r,int}} + \frac{D_{int} \cdot ln(D_{ext}/D_{int})}{2 \cdot k_{cc}} + \frac{1}{h_f} \right)^{-1} \tag{11}$$

$$\Delta T_{log} = \frac{\left(T_g^{TC2} - T_{f,out}\right) - \left(T_g^{TC11} - T_{f,in}\right)}{log\left(\left(T_g^{TC2} - T_{f,out}\right) - \left(T_g^{TC11} - T_{f,in}\right)\right)} \tag{12}$$

In equations (10) to (12), A_{int} is the combustor internal surface, k_{cc} is the cooling channel thermal conductivity, h_g is the convective heat transfer coefficient in the combustor, h_f is the convective heat transfer coefficient in the cooling channel, $h_{r,int}$ is the radiative heat transfer coefficient in the combustor[43] and T_g^{TC2} and T_g^{TC11} are the average gas temperature between position P1, P2 and P3 measured respectively at combustor base and at combustor outlet.

To calculate all the convective and radiative heat transfer coefficients, the thermodynamic properties, the transport properties and the velocities of the combustion gases in the combustion chamber must be known. Burned gases composition is obtained by numerical calculations with the IdealGasReactor module of the CANTERA package[44] using as chemical reaction mechanism the one developed by Dagaut et al.[45]. The thermodynamic and transport properties of each constituent of the burned gases are taken from literature[43,46]. The velocities of the combustion gases in the combustor are determined with CFD software Fluent, considering a 2-D axisymmetric domain. Turbulence is modeled by using the standard k-ε model, with standard wall functions near wall treatment.

III. Results and Discussion

A. Analysis of the Influence of Fuel Mass Flow Rate and Equivalence Ratio on Heat Transfer and on Combustor Cooling Efficiency

In this section, we detail the effects of $\dot{m}_f$ and φ variations on: i) the heat flux density passing from the combustion gases to the combustor wall, ii) the sensible heat flux absorbed by the fuel-coolant, iii) the heat transfer efficiency of the cooling system.

To investigate the influence of $\dot{m}_f$ and φ, test cases from 2 to 4 are examined. The operating conditions are given in table 1. As it can be seen in table 1, these experiments are carried out by varying fuel mass flow rate between 0.020 and 0.028 g.s^{-1}. As explained in section 2, during each test operating conditions are varied only when steady state has been achieved.

In fig. 4, the total heat flux densities passing from the combustion gases to the combustor wall at steady state (indicated as q_g) for experiments 2, 3, and 4 are given. Fig. 4 indicates that, independently from equivalence ratio, $\dot{m}_f$ increases always result in an increase in q_g whereas $\dot{m}_f$ decreases always results in a drop of q_g. Moreover, it proves that q_g

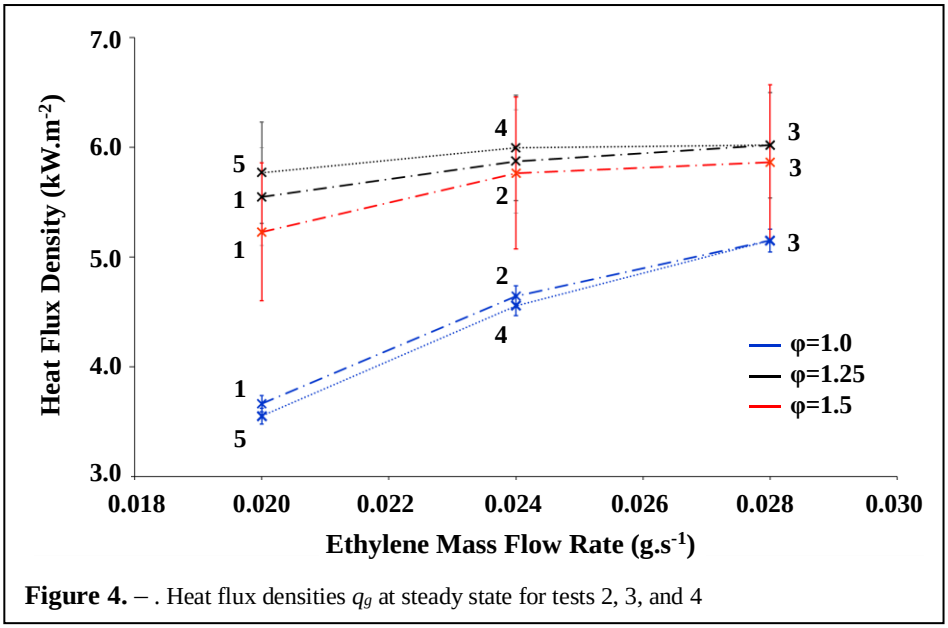

Figure 4. – . Heat flux densities q_g at steady state for tests 2, 3, and 4

increases and decreases are higher under stoichiometric conditions than under rich ones.

Fig. 4 also permits to understand the effect of φ on combustion gases-combustor wall heat transfers. Indeed, it shows that the total heat flux density q_g strongly increases when φ passes from 1.0 to 1.25 (depending on $\dot{m}_f$, it is between 16.8 to 62.4% higher). Conversely, a further raise of φ from 1.25 to 1.5 seems to produce the opposite result, i.e. a q_g drop. This finding is perhaps due to the fact that under fuel-rich conditions fuel combustion forms soot deposits and consequently the temperatures measured on the axis of the combustor are probably underestimated, due to the accumulation of soot aggregates on the thermocouples[40,47]. Thus, the calculated heat transfers from the burned gases to the combustion chamber surface are probably underestimated, the underestimation being greater when equivalence ratio is higher.

The formation of soot particles under fuel-rich conditions also explains why q_g increases with φ. In fact, due to the formation of carbon particles, even a small raise in φ results in a substantial increase in flame luminosity, as it can be seen in tab. 2, where the average flame emissivities ε_g are given for tests 2, 3, and 4. Hence, radiative heat transfer between the burned gases and the combustor wall, strongly depending upon flame emissivity, raises[36].

Test Case	Equivalence Ratio	Flame Emissivity
2	1.00	0.065 ± 0.004
3	1.25	0.123 ± 0.018
4	1.50	0.263 ± 0.040

Table 2. – Calculated flame emissivities at steady state for test cases number 2, 3, and 4

In fig. 5 and in fig. 6 the temperature achieved by the fuel-coolant at steady state at the outlet of the cooling channel (indicated as T_{hf}) and the sensible heat flux absorbed by the fuel-coolant at steady state divided by the cooling channel length (indicated as $q_{f,cc}$) are respectively given for cases 2, 3, and 4.

As already said in section 2, $q_{f,cc}$ is calculated using equation (9), even if probably temperature $T_{hf,}$ is not the highest one achieved by the coolant. This approach is questionable, as it leads to underestimate the real absorbed heat load. Moreover, it does not take into account the thermal energy absorbed by the endothermic decomposition reactions occurring in the cooling channel. Yet, it represents a first method to evaluate the performance of the cooling system and to compare tests run under different conditions.

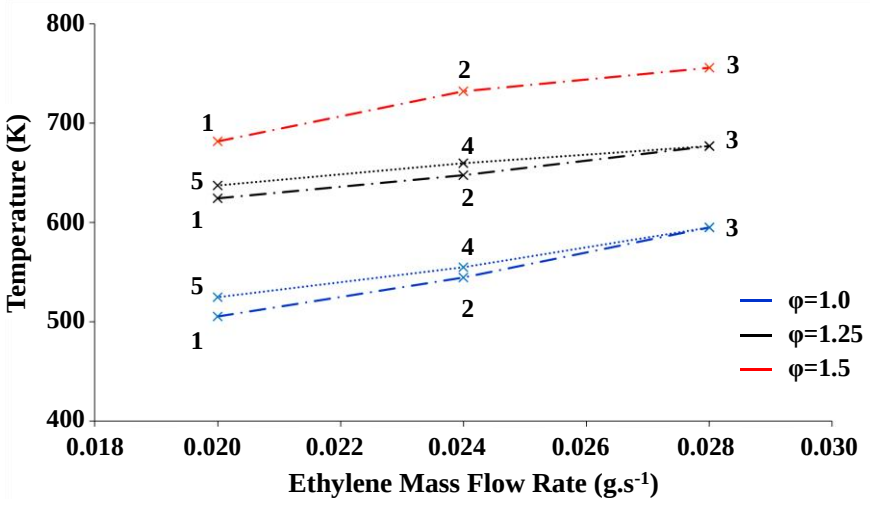

Figure 5. – T_{hf} at steady state for tests 2, 3, and 4

Fig. 5 indicates that a raise of $\dot{m}_f$ leads to a raise of T_{hf} whereas its drop leads to a decrease in T_{hf}. This is consistent with previous literature works[12,13]. Fig. 6 indicates that $\dot{m}_f$ raises lead to $q_{f,cc}$ increases whereas $\dot{m}_f$ decreases lead to $q_{f,cc}$ drops. This latter outcome is very important; indeed, it shows that a raise of the mass flow rate of the fuel fed to the combustor, which causes an increase in the heat flux density passing from the burned gases to the combustor internal wall (as seen in fig. 4), also results in the improvement of the cooling capability of the cooling system.

A hysteresis effect can be observed both in fig. 5 and in fig. 6 by comparing steady state 1 and steady state 5 and by comparing steady state 2 and steady state 4. This behavior had already been numerically predicted[12] and this experimental confirmation opens a new opportunity to study the characteristics times of the bench. This will be better developed in a future work.

To define the performance of the regeneratively cooled combustor, the heat transfer efficiency η of the overall cooling system has been determined for test cases 2, 3, and 4. They are given in table 3.

It can be observed that η grows as a function of $\dot{m}_f$ and φ. Hysteresis effects, due to system heat transfer dynamics, can be noted by comparing test 2 and test 3. Indeed, it can be seen that for both experiments the values reached by η at steady state 4 and 5 are always lower than those reached respectively at steady state 2 and 1. Table 3 also indicates that combustor performance generally grows with equivalence ratio.

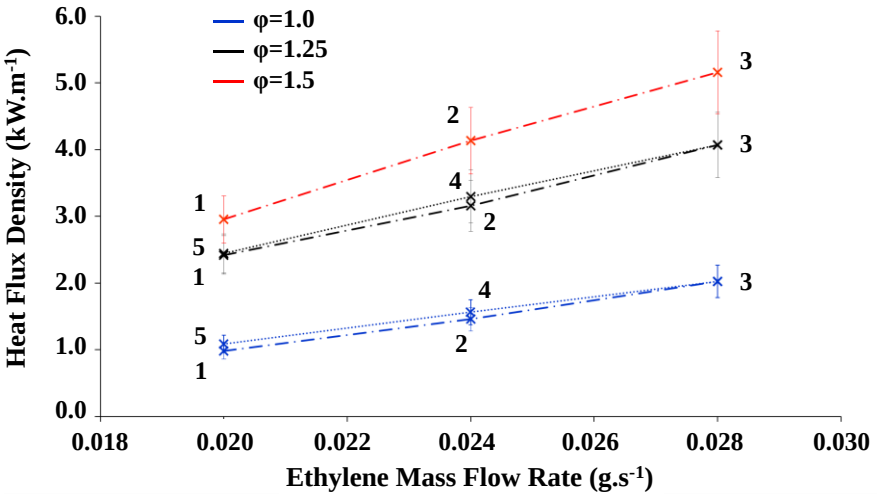

Figure 6. – Sensible heat flux $q_{f,cc}$ for tests 2, 3, and 4

These results are very relevant and confirm the findings based on the analysis of fig. 6, according to which both an increase in $\dot{m}_f$ and an increase in φ lead to the improvement of the cooling capability of the cooling system. Being, as explained above, the heat flux absorbed by the pyrolyzing fuel underestimated, the calculated heat transfer efficiencies are underestimated too.

Test Case	Equivalence Ratio	$\eta\|_{\dot{m}f = 0.020\ g/s}$	$\eta\|_{\dot{m}f = 0.024\ g/s}$	$\eta\|_{\dot{m}f = 0.028\ g/s}$	$\eta\|_{\dot{m}f = 0.024\ g/s}$	$\eta\|_{\dot{m}f = 0.020\ g/s}$
2	1.00	0.065±0.008	0.073±0.009	0.082±0.010	0.069±0.008	0.059±0.007
3	1.25	0.074±0.009	0.084±0.010	0.091±0.011	0.081±0.010	0.070±0.009
4	1.50	0.071±0.008	0.093±0.011	0.105±0.013	-	-

Table 3. – Combustor heat transfer efficiencies at steady state for tests 2, 3, and 4

B. Study of Fuel Coking Activity with the Description of Coking Monitoring Methods Suitable for Real-Time on-Board Application

As already observed, fuel thermal stability is a great challenge facing the use of endothermic hydrocarbon fuels. In order to investigate the consequences of fuel cooking activity on combustor dynamics, test case number 8 is now presented. This experiment has been stopped 332.4 minutes after the start as the coke deposits generated by fuel decomposition had caused the occlusion of the cooling channel.

The time-averaged carbon deposition rate along the cooling channel and the time-averaged cooling channel external wall temperature are given and in fig.7-a and 7-b. In order to calculate the time-averaged carbon formation rate, at test completion the rolled-up tube has been removed from the combustor washed with hexane and dichloromethane and dried with nitrogen. It has then been cut into 3 meters long pieces and the carbon accumulated in each section has been weighted with a precision balance (Kern ABS-N/ABJ-NM Analytical Balance). To express fuel coking rate in $\mu g.cm^{-2}.s^{-1}$, the measured coke mass has been divided by cooling channel internal surface and by test duration. This approach is questionable for two reasons. First, carbon coking activity is not uniform all over the experiment, as the temperatures achieved by the decomposing fuel vary with time. Second, it probably leads to underestimate the real carbon deposition rate, as during the first part of the experiment the temperatures achieved by ethylene in the cooling channel are too low to allow its pyrolysis. Nevertheless, it permits to obtain consistent results and to compare experiments run under different conditions. The cooling channel external wall temperature is calculated using the Dittus-Boelter correlation[48].

Fig. 7-a and 7-b indicate that carbon pyrolytic deposits only form in the highest temperature sections of the cooling channel, where the temperature achieved by its external surface is over 750 K, and that fuel deposition increases with increasing temperature. Following from the very high values of Reynolds number characterizing fuel flow in the

rolled-up tube (over 8000), it can be supposed that the difference of temperature between the decomposing hydrocarbon and the cooling channel wall is of few tens of degree K[49]. Being fuel residence time in the cooling channel for this test between 15.02±1.80 and 15.66±1.88 s, this outcome is consistent with the mainstream literature works, which states that, when few seconds residence times are considered, hydrocarbon pyrolytic deposition may only occur at temperatures over 700 K[7,31,33].

It can also be seen that the calculated coke formation rate seems to be higher in the last part of the cooling channel, between 40 and 45 meters from the inlet, even if the corresponding wall temperatures are slightly lower than the ones measured between 25 and 35 meters from the inlet. This result is probably attributable to the accumulation, in the last part of the rolled-up tube, of amorphous tar-like depositions that were generated in higher temperature zones and carried away by the flowing fuel. Due to their poor affinity to the solvents used to wash the tube before measuring its weight, it has not been possible to completely remove them. So, the computed values of coke formation rate between 35 and 40 meters from the inlet are overestimated.

The extent to which regenerative cooling benefits can be capitalized is not only related to our ability to moderate coke formation, but also to the development of carbon deposition monitoring methods suitable for real-time on-board application. In this sense, the monitoring of fuel-coolant pressure drop in the cooling channels (ΔP_f) could be a viable strategy. In fig. 8, ΔP_f is given as a function of time for test 8.

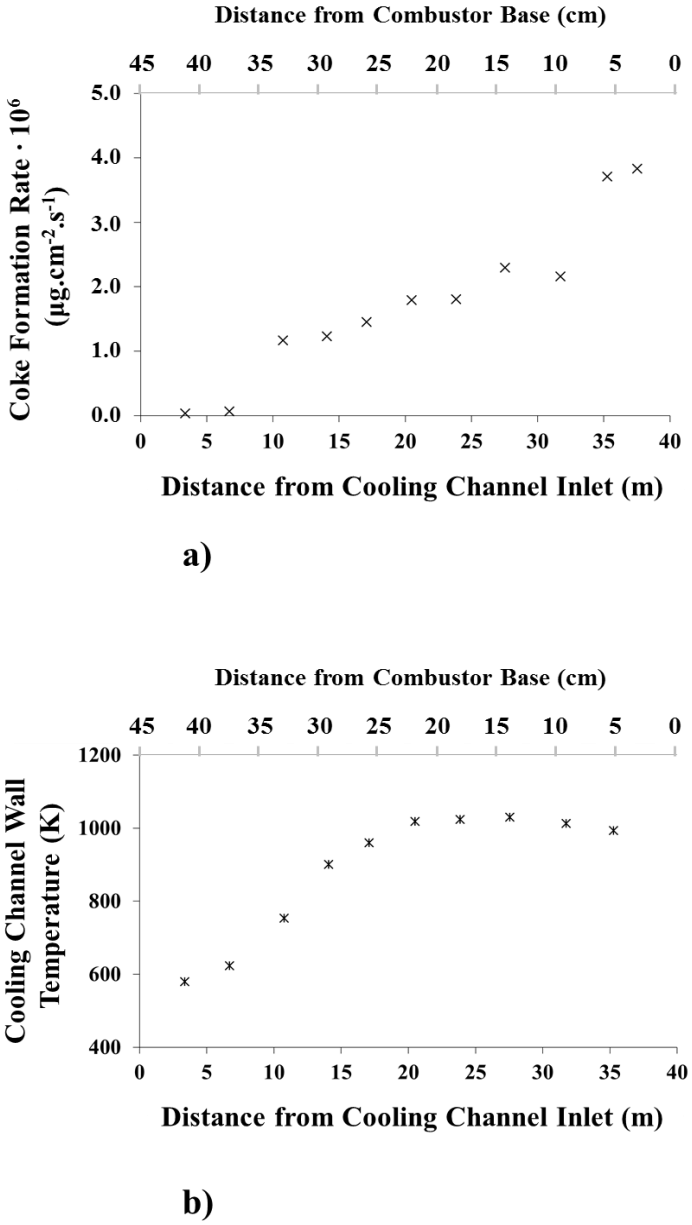

Figure 7. – Comparison between coke formation rate (a) and cooling channel wall temperature (b) for test 8

The two very abrupt pressure loss increases indicated as $\Delta P_{f,1}$ and $\Delta P_{f,2}$ result from fuel mass flow rate raises (respectively from 0.020 to 0.024 g;s^{-1} and from 0.024 to 0.028 g.s^{-1}), whereas the brusque pressure loss decrease indicated as $\Delta P_{f,3}$ is attributable to fuel flow rate reduction from 0.024 to 0.020 g.s^{-1}. Instead, the progressive pressure drop increases $\Delta P_{f,b1}$ and $\Delta P_{f,b2}$ are both due to the gradual accumulation of coke deposits on the cooling channel internal surface, which reduces the tube cross section. As already said, this test was run until the final sudden fuel pressure drop raise that can be easily seen in the figure, indicating that complete blockage was imminent

IV. Conclusion

Regenerative cooling is expected to guarantee the thermal protection of Scramjet propelled vehicles flying at velocities over Mach 5. Its effectiveness is studied in this paper when an endothermic hydrocarbon fuel is used. A regeneratively cooled combustor, allowing the experimental study of pyrolysis-combustion coupling and fuel coking activity, has been developed. It is used to run tests under both stationary and transient conditions using ethylene as fuel and air as oxidizer. The influence of two major parameters, i.e. fuel mass flow rate and equivalence ratio, on the heat flux density passing from the combustion gases to the combustor wall, on the sensible heat flux absorbed by the fuel-coolant, and on combustor heat exchange efficiency has been determined. It has been observed that an increase in fuel mass flow rate and equivalence ratio leads to a general raise of the heat flux density between the burned gases and the internal surfaces of the combustion chamber. It has been illustrated that mass flow rate and equivalence ratio increases also result in an increase in the thermal energy absorbed by the coolant; this means that the cooling capability of the cooling system grows as a function of the two operating parameters. It has also been seen that the heat exchange efficiency of the combustor increases with equivalence ratio whereas it decreases with fuel mass flow rate. The effects of fuel coking activity on the cooling system have been examined. It has been proved that, when fuel-coolant residence time in the cooling channel is about 15 s, the fuel starts to form carbon deposition in the cooling channel in a temperature range of 700-750 K. A fuel coking activity monitoring method suitable for real-time on-board application, i.e. the measure of fuel pressure drop in the cooling channels, has been defined and tested. The knowledge acquired in this paper represents a first step to better understand the effect of the command parameters on the dynamics of a regeneratively cooled combustor. It will now be possible in a future work to develop analytical relationships for an engine control strategy to generate a required thrust without exceeding a temperature threshold.

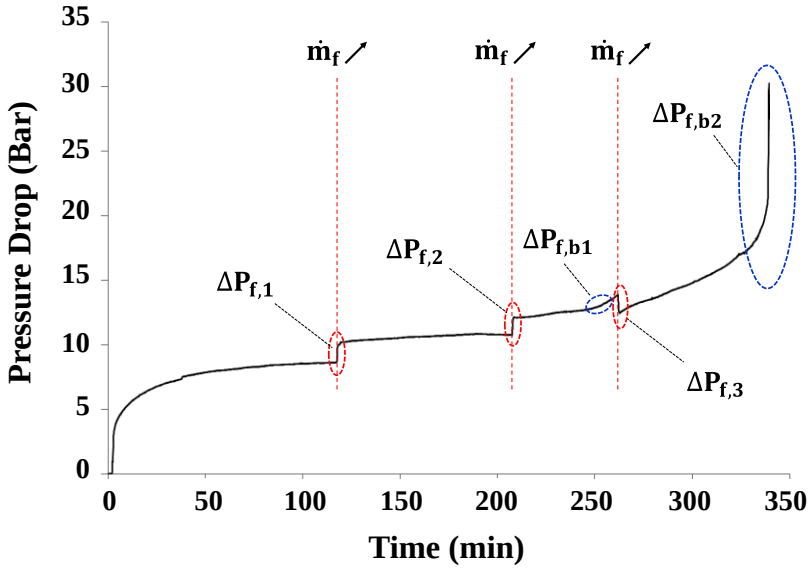

Figure 8. – Fuel pressure drop in the cooling channel as a function of time for test case 8

References

[1] Van Wie D. M., D'Alessio S. M., and White M. E. "Hypersonic Air breathing Propulsion," *Johns Hopkins APL Technical Digest*, vol. 26, 2005, pp. 430–436.

[2] Fry, R. S., "A Century of Ramjet Propulsion Technology Evolution," *Journal of Propulsion and Power*, vol. 20, 2004, pp. 27–58.

[3] Curran, E. T., "Scramjet Engines: The First Forty Years," *Journal of Propulsion and Power*, vol. 17, 2001, pp. 1138–1148.

[4] Van Griethuysen, Glickstein, M. R., Petley, M. R., Gladden D. H., and Kubik, D. L., "High-Speed Flight Thermal Management", *Developments in High-Speed Vehicle Propulsion Systems, in Progress in Aeronautics and Astronautics*, vol. 165, 1996, pp. 517-579.

[5] Ulas, A., and Boysan, E., "Numerical analysis of regenerative cooling in liquid propellant rocket engines," *Aerospace Science and Technology*, vol. 24, 2013, pp. 187–197.

[6] Hou, L. Y., Dong, N., and Sun, D. P., "Heat transfer and thermal cracking behavior of hydrocarbon fuel," *Fuel*, vol. 103, 2013, pp. 1132–1137.

[7] Maurice, L., Edwards, T., and Griffits, J., "Liquid Hydrocarbon Fuels for Hypersonic Propulsion," in *Scramjet Propulsion, Progress in Aeronautics and Astronautics*, vol. 189, 2001, pp. 757-822.

[8] Heiser, W. H., and Pratt, D. T, "Hypersonic Air-breathing Propulsion", edited by J.S. Przemieniecki, in *Progress in Astronautics and Aeronautics*, Washington DC, 1994.

[9] Bao, W., Li, X., Qin, J., Zhou, W., and Yu, D., "Efficient Utilization of Heat Sink of Hydrocarbon Fuel For Regeneratively Cooled Scramjet," *Applied Thermal Engineering*, vol. 33-34, 2012, pp. 208–218.

[10] Bouchez, M., "Scramjet Thermal Management Scramjets or Dual Mode Ramjets for High Speed Atmospheric Flight," NATO Science and Technology Organization, 2010.

[11] Sobel, D. R., and Spadaccini, L. J., "Hydrocarbon Fuel Cooling Technologies for Advanced Propulsion," *Journal of Engineering for Gas Turbines and Power*, vol. 119, 1997, pp. 344-351.

[12] Gascoin, N., and Gillard, P., "Dynamic Study of Coupled Heavy Hydrocarbon Pyrolysis and Combustion," *Combustion Science and Technology*, vol. 184, 2012, pp. 2136–2153.

[13] Taddeo, L., Gascoin, N., Fedioun, I., Chetehouna, K., Lamoot, L., and Fau, G., "Dimensioning of automated regenerative cooling: Setting of high-end experiment," *Aerospace Science and Technology*, vol. 43, 2015, pp. 350–359.

[14] Drummond, J. P., Bouchez, M., McClinton, "CHAPTER 1: OVERVIEW OF NATO BACKGROUND ON SCRAMJET TECHNOLOGY," Technologies for Propelled Hypersonic Flight, NATO Science and Technology Organization, 2010.

[15] Gascoin, N., Gillard, P., Dufour, E., and Touré, Y., "Validation of Transient Cooling Modeling for Hypersonic Application," *Journal of Thermophysics and Heat Transfer*, vol. 21, 2007, pp. 86–94.

[16] Kirchberger, C., Wagner, R., Kau, H-P., Soller, S., Martin, P., Bouchez, M., and Bonzom, C., "Prediction and Analysis of Heat Transfer in Small Rocket Chambers," *46th AIAA Aerospace Sciences Meeting and Exhibit*, Reno, January 7-10, 2008.

[17] Dufour, E., and Bouchez, M., "Post-Experimental computations of a kerosene-fueled scramjet", *10th AIAA/NAL-NASDA-ISAS International Space Planes and Hypersonic Systems and Technologies Conference*, Kyoto, Japan, April 24-27, 2001.

[18] Frankel, J. I., Keyhani, M., Elkins, B., and Arimilli, R. V., "New In Situ Method for Estimating Thermal Diffusivity Using Rate-Based Temperature Sensors," *Journal of Thermophysics and Heat Transfer*, vol. 24, 2010, pp. 811–817.

[19] Parris, D. K., and Landrum, D. B., "Effect of Tube Geometry on Regenerative Cooling Performance," *41st AIAA/ASME/SAE/ASEE 41st Joint Propulsion Conference and Exhibit*, Tucson, Arizona, July 10-13, 2005.

[20] Yagley, J., Feng, J., and Merkle, C. L., "The effect of Aspect Ratio on the Effectiveness of Combustor Coolant Passages," *AIAA/SAE/ASME/ASEE 28th Joint Propulsion Conference and Exhibit*, Nashville, Tennessee ,July 6-8, 1992.

[21] Bao, W., Qin, J., Zhou, W. X., and Yu, D. R., "Effect of cooling channel geometry on re-cooled cycle performance for hydrogen fueled scramjet," *International Journal of Hydrogen Energy*, vol. 35, 2010, pp. 7002–7011.

[22] Wadel, M.F., "Comparison of High Aspect Ratio Cooling Channel Designs for a Rocket Combustion Chamber," *AIAA/ASME/SAE/ASEE, 33rd Joint Propulsion Conference*, Seattle, July 06-09, 1997.

[23] Pizzarelli, M., Nasuti, F., and Onofri, M., "Trade-off analysis of high-aspect-ratio-cooling-channels for rocket engines," *International Journal of Heat and Fluid Flow*, vol. 44, 2013, pp. 458–467.

[24] Medwick, D.G., Castro, J.H., Sobel, D.R., Boyet, G., Vidal, J.P., "Direct fuel cooled composite structure" *XIV International Symposium on Air Breathing Engines (ISABE)*, Florence, September 5-10, 1999.

[25] Peres, P, Lansalot, J., Bouchez, M., and Saunier, E. "Advanced carbon-carbon injection struts for actual scramjet," *AIAA Space Plane and Hypersonic Systems and Technology Conference*, Norfolk, Virginia, November 18-22, 1996.

[26] Johnson, S.J., Adharapurapu, R.R., Pollock, T.M., "Post-Fabrication Vapor Phase Strengthening of a Nickel-Based Sheet Alloy for Thermo-Structural Panels," *Acta Materialia*, vol. 56, 2008, pp. 4577-4584.

[27] Evans, A. G., Zok, F. W., Levi C. G., McMeeking, R. M., Miles, R. M., and Pollock, T. M., "Revolutionary materials for hypersonic flight," University of California Final Technical Report, October 2011.

[28] Falempin, F., "The French PROMETHEE Program on Hydrocarbon Fueled Dual Mode Ramjet: Status in 2001," *AIAA/CIRA 13th International Space Planes and Hypersonics Systems and Technologies*, Capua, May 16-20, 2005.

[29] Daniau, E., and Sicard, M., "Experimental and numerical investigations of an endothermic fuel cooling capacity for scramjet application," *AIAA/CIRA 13th International Space Planes and Hypersonics Systems and Technologies*, Capua, May 16-20, 2005.

[30] Vincent-Randonnier, A., Rouxel, B., Roux, P., Poirot, M., Sicard, M., Raepsaet, B., and Ser, F., "Experimental Investigations on the Self-Ignition of a Thermally Decomposed Endothermic Fuel in Hot Supersonic Air Flow in the MPP-LAERTE Combustion Test Bench," *15th AIAA International Space Planes and Hypersonic Systems and Technologies Conference*, Dayton, Ohio, April 28 – May 1, 2008.

[31] Chin, J. S., and Lefebvre, a. H., "Influence of Flow Conditions on Deposits from Heated Hydrocarbon Fuels," *Journal of Engineering for Gas Turbines and Power*, vol. 115, 1993, pp. 433-438.

[32] Sobel, D. R., and Spadaccini, L. J., "Hydrocarbon Fuel Cooling Technologies for Advanced Propulsion," *Journal of Engineering for Gas Turbines and Power*, vol. 119, 1997, pp. 344-351.

[33] Spadaccini, L. J., Sobel, D. R., and Huang, H., "Deposit Formation and Mitigation in Aircraft Fuels," *Journal of Engineering for Gas Turbines and Power*, vol. 123, 2001, pp. 741-746.

[34] Gascoin, N., Gillard, P., Bernard, S., and Bouchez, M., "Characterization of coking activity during supercritical hydrocarbon pyrolysis," *Fuel Processing Technology*, vol. 89, 2008, pp. 1416–1428.

[35] Sicard, M., Raepsaet, B., Ser, F., and Masson, C., "Thermal decomposition of a model endothermic fuel. Preliminary study before testing in the MPP-LAERTE supersonic combustion test bench," *14th AIAA/AHI Space Planes and Hypersonic Systems and Technologies Conference*, Canberra, Australia, November 6-10, 2006.

[36] Perry, R. H., & Green, D. W., "Heat Transfer By Convection", *Perry's chemical engineers' handbook, vol. 5, Heat and Mass Transfer*, McGraw-Hill, 2008.

[37] Baukal, C. E., "Heat Transfer", *Industrial burners handbook, vol. 2*, Industrial Combustion Series, 2004, pp. 14-31.

[38] Mulholland, G. W., and Croarkin, C., "Specific extinction coefficient of flame generated smoke", *Fire and Materials*, vol. 24, 2000, pp. 227–230.

[39] Ciajolo, A., D'Anna, A., Barbella, R., Tregrossi, A., and Violi, A., "The effect of temperature on soot inception in premixed ethylene flames," *Symposium (International) on Combustion*, vol. 26, 1996, pp. 2327–2333.

[40] Russo, C., Alfe, M., Rouzaud, J. N., Stanzione, F., Tregrossi, A., and Ciajolo, A., "Probing structures of soot formed in premixed flames of methane, ethylene and benzene," *Proceedings of the Combustion Institute*, vol. 34, 2013, pp. 1885–1892.

[41] Harris, S. J., and Weiner A. M. "Soot particle inception and O_2 profiles in a premixed ethylene flame," *Combustion and Flame*, vol. 66, 1986, pp. 211–214.

[42] Fakheri, A., "Heat Exchanger Efficiency," *Journal of Heat Transfer*, vol. 129, 2007, pp. 1268-1276.

[43] Hottel, H. C., Noble J. J., Sarofim A. F., Silcox G. D., Wankat P. C., Knaeble K. S., "Heat and Mass Transfer," *Perry's Chemical Engineers' Handbook*, *vol.* 5, edited by Perry, R. H., and Green, D. W, New York, McGrow-Hill, 2008, pp. 7-43.

[44] Goodwin, D. G., Moffat, H. K., and Speth, R. L., "Cantera: An object- oriented software toolkit for chemical kinetics, thermodynamics, and transport processes," http://www.cantera.org, 2016, Version 2.2.1.

[45] Dagaut, P., Boettner, J. C., and Cathonnet, M., "Ethylene pyrolysis and oxidation: A kinetic modeling study," *International Journal of Chemical Kinetics*, vol. 22, 1990, pp. 641–664.

[46] Poling, B. E., Thomson, G. H., Friend, D. G., Rowley, R. L., Wilding, W. V., "Physical and Chemical Data," *Perry's Chemical Engineers' Handbook*, *vol.* 2, edited by Perry, R. H., and Green, D. W, New York, McGrow-Hill, 2008, pp. 156-182, 185-202, 420-463.

[47] Álisson, A., and Santos, B., "Evaluation of the Influence of the Soot Deposition on Thermocouple Measures in Combustion Experiment," VI National Congress of Mechanical Engineering, Campina Grande, Brazil, 2010.

[48] Xuan, Y., and Li, Q., "Investigation on convective heat transfer and flow features of nano-fluids," *Journal of Heat Transfer*, vol. 125, 2003, pp. 151-155.

[49] Gascoin, N., Gillard, P., Bernard, S., Abraham, G., Bouchez, M., and Daniau, E. T., "Measurements for fuel reforming for scramjet thermal management and combustion optimization : status of the COMPARER project," 14th AIAA/AHI Space Planes and Hypersonic Systems and Technologies Conference, Canberra, Australia, November 6-9, 2005.